Article no. 12

THE CIVIL ENGINEERING JOURNAL 2-2020

THE EFFECT OF CONCRETE-STEEL INTERFACE MODEL ON FINITE ELEMENT ANALYSIS OF CONCRETE FILLED SQUARE STEEL TUBE BEAM

Mahmud Kori Effendi

Department of Civil Engineering, Faculty of Civil Engineering and Planning, Universitas Islam Indonesia (UII), Indonesia; kori.effendi@uii.ac.id

ABSTRACT

Three-dimensional nonlinear finite element (FEA) is developed to predict the experimental behaviour of concrete filled square steel tubular member. The FEA is conducted to determine moment carrying capacity at ultimate load for simple beam. The concrete-steel interface model is the important parameter affecting the result of FEA simulation. Based on the experimental result, there is a local buckling near the loading contact point. To investigate the local buckling phenomenon, concrete-steel interface model is studied by using contact analysis between concrete and steel elements, by using rigid bar element (rbe2 element) and by using interface elements. The geometrical non-linearity, material non-linearity, loading, boundary conditions is the same for all analysis models. To account for all of these properties, FEA model by means MSC Marc Mentat software is developed. The proposed model can predict the ultimate strength with difference only 5-30%. The collapse modes by FEA model are also compared. Based on the numerical analysis, it can be seen that the local buckling is clearly shown in the FEA model with the concrete and steel interface by using interface elements.

KEYWORDS

Concrete filled steel tube, Finite element analysis, Concrete-steel interface

INTRODUCTION

Concrete filled steel tubes (CFST) are composite members comprise of steel tubes with concrete infill. It became popular for modern structural projects. Its ductility is better than conventional structures such as steel and reinforced concrete structures [1-3]. The concrete infill restrains inward buckling of the steel tube, while the steel tubes act as tensile reinforcement for the concrete infill. Studies on flexural behaviour of CFST beam have been conducted by many researchers [4-6]. The concrete infill improves the flexural strength and ductility of structural members of CFST beam as well as to prevent local buckling of steel tubes [7]. A series of experiments of CFST beam with D/t ratios ranging from 74 to 110 is conducted to examine geometrical instabilities.

Finite element analysis (FEA) has been used by many researchers to study the behaviour of CFST beams under pure bending. Karrech et al [8] conducted FEA of cold-formed Circular Hollow Section (CHS) beams filled with concrete subjected to a static plastic pure bending. A damaged plasticity model with softening effect was used for concrete and Von-Miseselasto-plasticity with hardening was used for steel. Three dimensional FEA of concrete filled steel tubes has been used by many researchers, by using ANSYS software [9-11] and by ABAQUS software [12-14].

A Three-dimensional nonlinear finite element (FEA) is developed to predict the experimental behaviour of concrete filled square steel tubular member by using MSC Software, MSC Marc-Mentat [15]. The FEA is conducted to determine moment carrying capacity at ultimate load for simple beam. The concrete and steel material model is modelled by using the nonlinear material. The nonlinear geometry is conducted by means of large displacement analysis. The result of the three-dimensional finite element analysis is then verified against the experimental results by Effendi [16].

The concrete-steel interface model is the important parameter affecting the result of FEA simulation. A Three-dimensional nonlinear finite element (FEA) is developed to predict the experimental behaviour of concrete filled square steel tubular member. The FEA is conducted to determine strength for CSFT simple beam.

EXPERIMENTAL PROGRAM

In order to verify the proposed model, one specimen in total had been tested. The detail of specimen in the experimental study has been shown in Table 1.

Material Properties

The test specimen of square tube, Sfs (B/t=33.2), had been tested at the Department of Architecture, Kyushu University [16]. Square shapes of cross section of steel tubular members as well as the specimen length and the position of loading which was analysed in this study is shown in Figure 1. The yield stress of square tubular members was 385 N/mm^2. The Poisson's ratio, v is 0.3. Table 1 summarizes the dimensions and material properties.

Experimental Set-up

The test setup for static loading is illustrated in Figure 2. The supports were pin and roller supports at both ends. Roller support was a simple one which was just greased between the bottom end plate of a specimen and testing bed which was made by H-shaped steel, so that specimen ends can freely slide in the member axis direction.

Two displacement transducers were installed to measure the displacement of a loading head, and a laser displacement sensor was placed at the bottom of the mid-span of a tubular member to measure the overall displacement. Strain gauges were installed at the bottom of the mid and quarter span for a square tube.

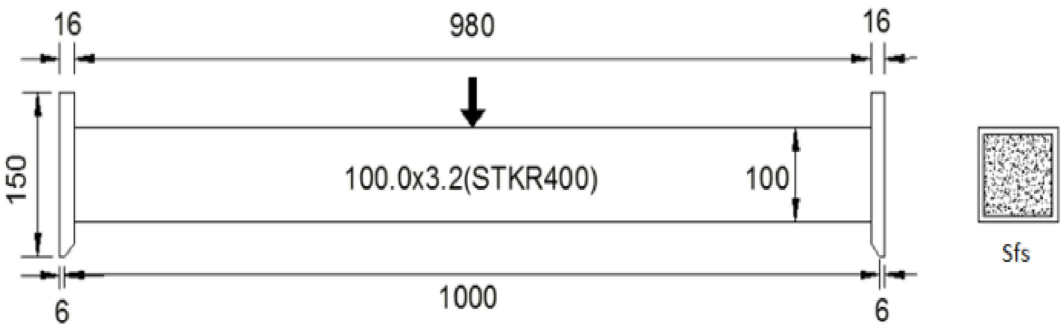

Fig. 1 – Specimen's Illustration (unit: mm)

DOI 10.14311/CEJ.2020.02.0012

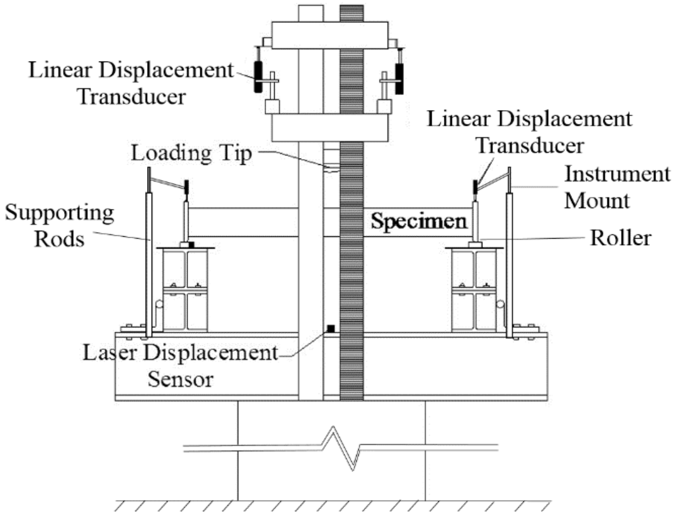

Fig. 2 – Experimental Setup

Tab. 1 - Measured Dimensions and Material Properties of Specimen

Name of Specimen	Steel Tube				Concrete	
	${}_sB$ (mm)	t (mm)	f_y (N/mm^2)	E_s (N/mm^2)	${}_c\sigma_B$ (N/mm^2)	E_c (N/mm^2)
Sfs	100.0	3.01	385	188000	71.5	39900

FINITE ELEMENT ANALYSIS

In this study, the commercial software package, MSC Marc-Mentat is used. MSC Marc, general-purpose finite element software, has been used as the analytical tool. MSC Mentat was employed to generate the mesh, material and geometry assignment, loading conditions and boundary conditions. FEM analysis can simulate accurately the response of structure under static loading if the model is used properly. The validity of FEM analysis was justified by comparing with the experimental results. The full Newton-Raphson iterative procedure is chosen to solve the iteration process. The iterative procedure is terminated when the convergence ratio is less than criterion of tolerance, residual checking and displacement checking.

Material Model

MSC Marc [14] requires the stress and strain characteristics to be entered as the true stress and the equivalent plastic strain, respectively. The tensile strength of steel tubes taken from tensile test is represented as in Figure 3. The von Mises yield criterion and the kinematic hardening rule are used as the plastic flow conditions.

The infill concrete is simulated by implementing the Mohr-Coulomb yield criterion combined with the isotropic hardening rule. The concrete model in compressive path is as shown in Figure 4. The tensile model is the cracking stress specified to be a very small value and the tension softening modulus specified to almost zero. The Poisson’s ratio is assumed as 0.2.

DOI 10.14311/CEJ.2020.02.0012

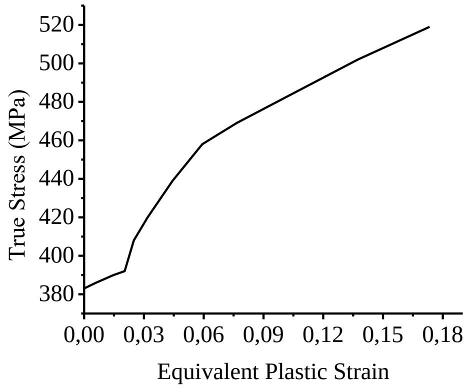

Fig. 3 – .Equivalent Plastic Strain and True Stress Relationships of Steel Tubes

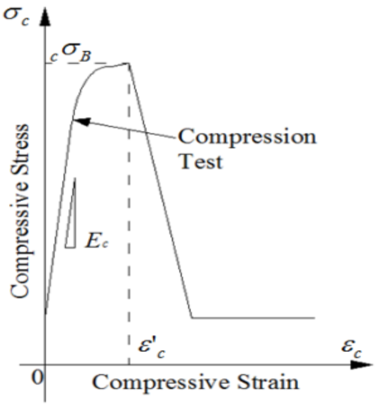

Fig. 4 – Concrete Model in Compressive Path

Element Type, Boundary Conditions and Mesh Segmentation

The FEA model with contact option can be seen in Figure 5 and with interface element can be seen in Figure 6. Both models use the eight-node solid, isoparametric, arbitrary hexahedral element with three degrees of freedom per a node (*u*, *v* and *w*), (the element type 7 of MSC Marc [17], for the analytical model of a steel tubular and concrete elements. While, FEA model with rbe2 element can be seen in Figure 7. The steel used the element type 75 of MSC Marc. The element is a four-node, thick-shell element with global displacements and rotations as degrees of freedom. The coordinates, displacements and the rotations use bilinear interpolation.

The supporting conditions were the simple beam to which the concentrated lateral load applied at the mid-span. The all nodes on both supports were constrained in the direction of *Y* axis and an additional one node in the mid of the nodes were constrained in the direction of *Z* axis to stabilize the analysis. The remaining degrees of freedom were set to be free.

The displacements of one node at the bottom of cross section at mid span were constrained in the direction of *X* axis. The loading tip, which is a rigid body composed of rigid surface elements, applies lateral loads to a steel tube that was composed of deformable elements. The vertical displacement of the loading tip was increased by the displacement control method. With respect to end plate, the shell elements are used with the elastic material properties.

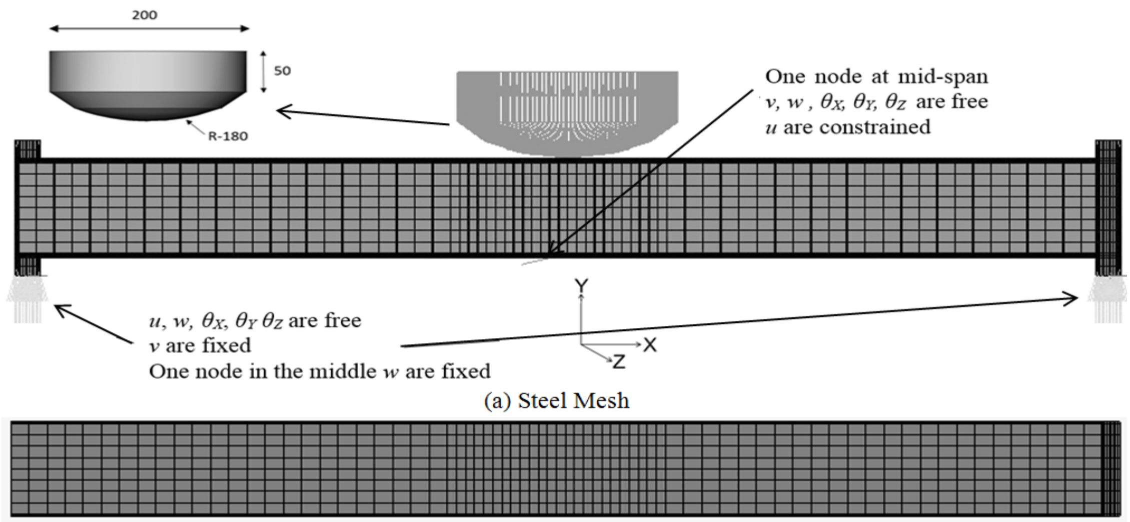

(a) Steel Mesh

(b) Concrete Mesh

Fig. 5 – Boundary Conditions and Mesh Segmentation with Contact Analysis

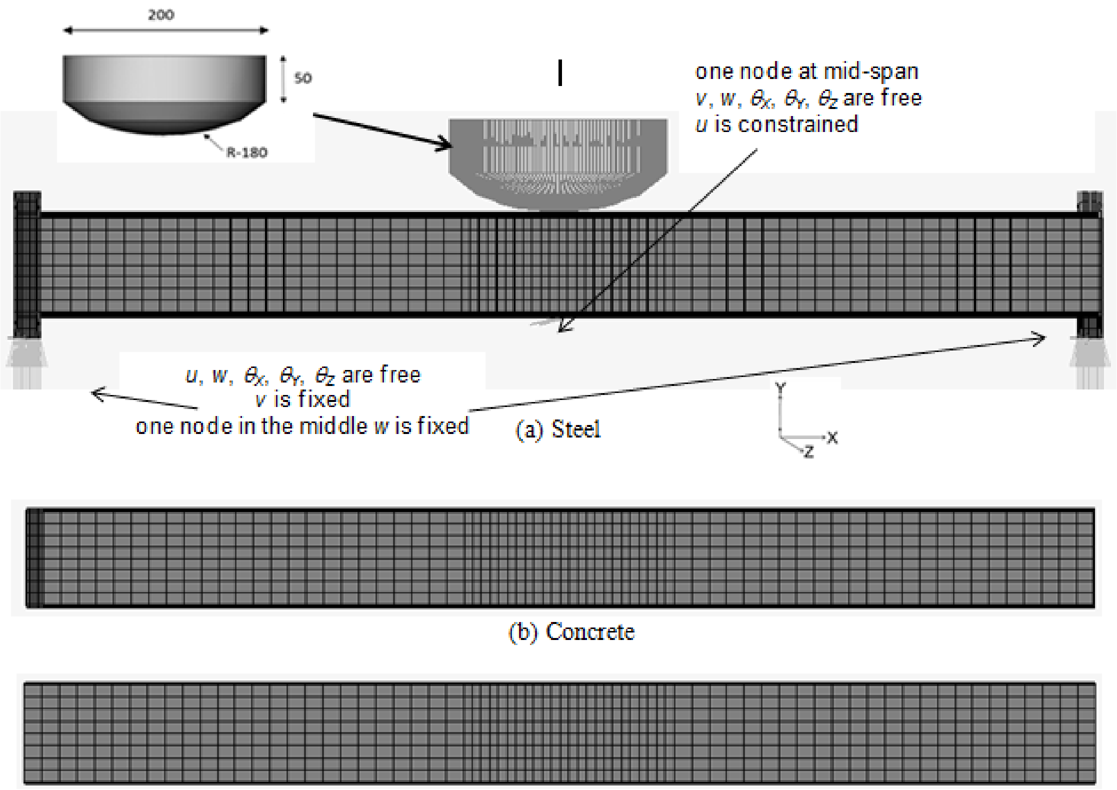

(a) Steel

(b) Concrete

(c) Interface element

Fig. 6 – Boundary Conditions and Mesh Segmentation with Interface Element

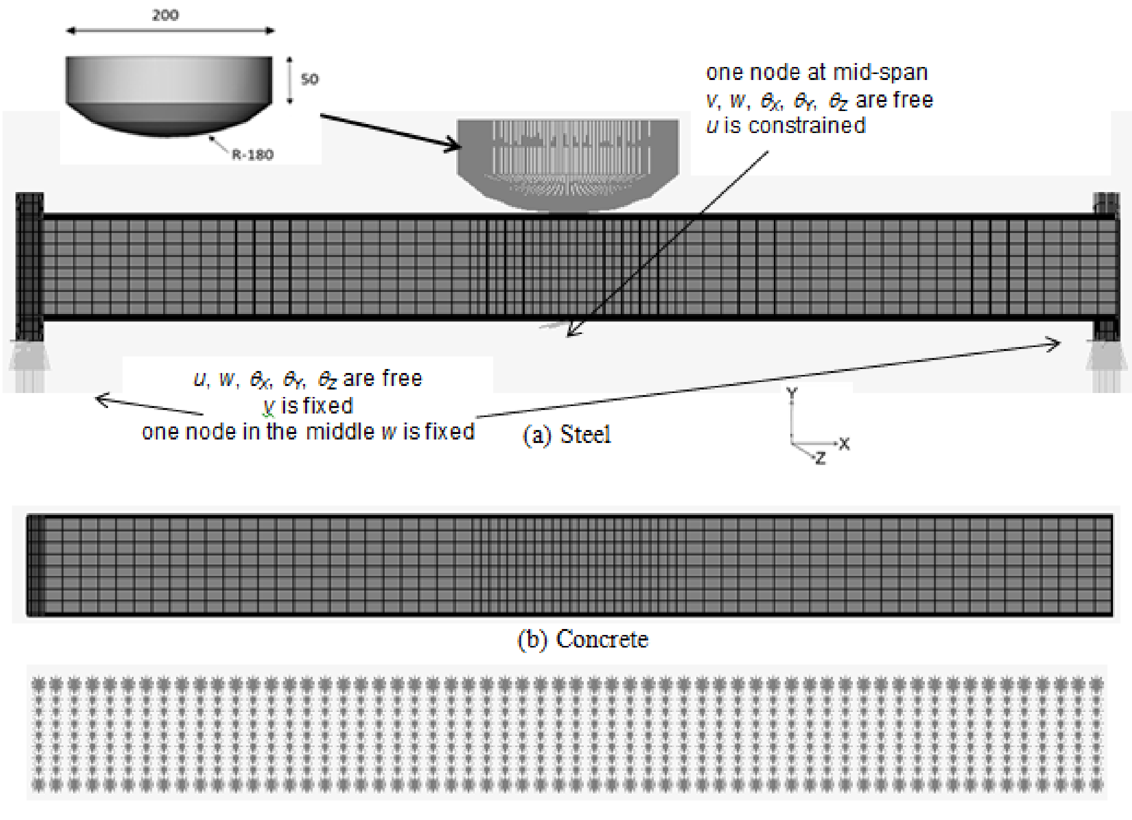

(c) rbe2 element

Fig. 7 – Boundary Conditions and Mesh Segmentation with rbe2 element

Contact Analysis

The contact interactions are considered between a rigid body of the loading tip and a deformable body of steel tubular member as well as between steel tubular elements and concrete elements. The contact tolerance of the deformable body was defined to be between plus and minus of 0.1 mm. The MSC Marc deals with the contact analysis by the direct constraint procedure.

Interface Element

The interface element is set between steel elements and concrete elements. The element type 188 of MSC Marc [18], an eight-node three-dimensional interface element, is used to simulate the onset and progress of delamination. The connectivity of the element is shown in Figure 8 where the nodes 1, 2, 3 and 4 correspond to the bottom of the interface and nodes 5, 6, 7 and 8 to the top. The bottom of the interface side is contact with the concrete element and the top is contact with the steel element. The stress components of the element are one normal traction and two shear tractions, which are expressed with respect to the local coordinate system, indicated in Figure 8.The corresponding deformations are the relative displacements between the top and the bottom face of the element. The element is set to be infinitely thin or zero thickness, in which case the faces 1-2-3-4 and 5-6-7-8 coincide.

DOI 10.14311/CEJ.2020.02.0012

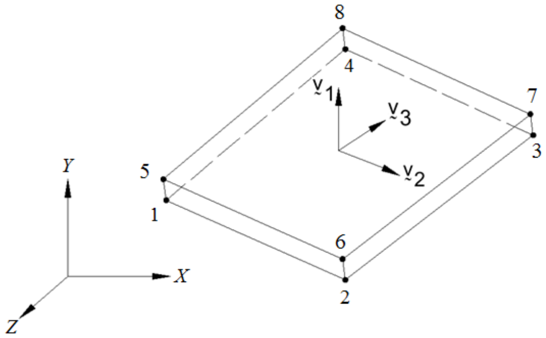

Fig. 8 – The connectivity of the interface element

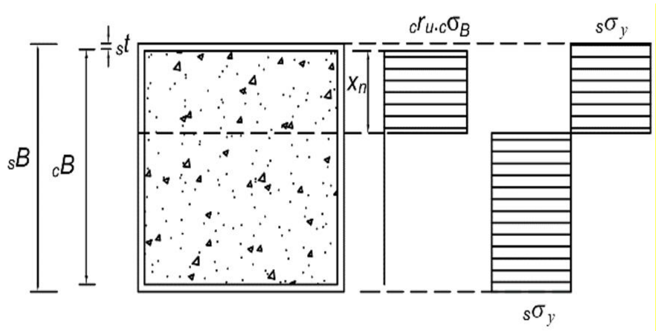

Fig. 9 – Stress Block for CFST Members' Ultimate Bending Capacity

Rigid Bar Element

The rigid bar element (rbe2 element) can be used for connecting two nodes to model a pinned connection with 3 translational DOFs. The connection is between a single retained node with dependent degrees of freedom specified at an arbitrary number of tied nodes. These elements artificially add stiffness by constraining the system to follow a one to one linear displacement and/or rotational relationship between the connected nodes. The distance between the tied nodes to the retained node must be greater than zero. The updated Lagrange is set and large rotation formulation is automatically used in the analysis.

THEORETICAL BACKGROUND

The theoretical value of the ultimate moment, M_u which is the full plastic moment of a CFST member, is based on the Recommendations by AIJ [19], where the stress distributions are assumed as shown in Figure 9. The neutral axis, x_n is obtained by trial and error so the sum of ultimate axial force, Equation (1) close or equal to zero. Then, M_u can be calculated from Equation (2). The concrete and steel tubes contribution in ultimate axial force calculation is determined by Equation (3) and Equation (5). The concrete and steel tubes contribution in ultimate moment is determined by Equation (4) and Equation (6). It was assumed that there was no concrete strength reduction so the value of ${}_c r_u$, reduction factor for concrete strength, is set equal to 1.

$$N_u = {}_c N_u + {}_s N = 0 \tag{1}$$

$$M_u = {}_c M_u + {}_s M_u \tag{2}$$

$${}_c N_u = x_n \cdot {}_c B \cdot {}_c r_u \cdot {}_c \sigma_B \tag{3}$$

$$ {}_cM_u = \frac{1}{2}\left({}_cB - x_n\right).x_n \cdot {}_cB \cdot {}_cr_u \cdot {}_c\sigma_B \tag{4} $$

$$ {}_sN_u = 2.\left(2.x_n - {}_cB\right).{}_st \cdot {}_s\sigma_y \tag{5} $$

$$ {}_sM_u = \left[\left({}_sB - {}_st\right).{}_sB + 2.\left({}_cB - x_n\right).x_n\right].{}_st \cdot {}_s\sigma_y \tag{6} $$

The theoretical value of the ultimate strength, P_u, is calculated based on the equilibrium of simple beam as Equation (7). The ultimate strength by FEA and experiment are defined as the point at which the tangent stiffness of the load-deflection curve becomes one-sixth of the initial stiffness as shown in Figure 10 [20].

$$ P_u = 4M_u / L \tag{7} $$

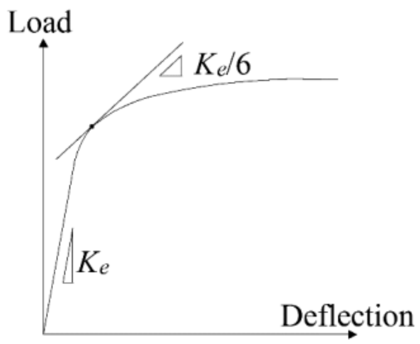

Fig. 10 – Definition of Ultimate Strength by Experimental

RESULTS AND DISCUSSION

Comparison of Load-Deflection Relationships by Experiments and by Finite Element Analysis

In Figure 11, it is seen that the load-deflection curve of the FEA in the elastic range is similar as that of experimental results. However, after the elastic behaviour is extended the FEA using contact analysis is almost the same as that of experimental results. FEA using interface element and using rbe2 element are stiffer than FEA using contact analysis in the initial slope. After the yielding of the steel tube is extended, FEA using rbe2 element did not show strength degradation. The strength is increasing as the deflection is increasing. The rbe2 element increases the stiffness of the specimen.

The dot mark shows the ultimate strength both FEA and experiment. The ultimate strength resulted from the FEA using contact analysis, interface element and rbe2 element have a different value to the theoretical value of the experimental load with 6.5%, 16.7% and 27.3%, respectively as shown in Table 2. While, the ultimate strength resulted from the experimental has a difference value to the theoretical value of the experimental load with 9.3% as shown in Table 2.This proves that the theoretical value is safe for the CFST beam.

Comparison of Load-Strain Relationships by Experiments and by Finite Element Analysis

The strain is taken from the mid of midspan of the specimen. In Figure 12, it is seen that the elastic range of FEA using rbe2 element is stiffer than others. It is caused by the additional stiffness from the rbe2 element. The strain from FEA using interface element is the same as that of experiment. The strain from FEA using contact analysis is the same as that of experimental in the elastic range, however in the plastic range the strain is lower than that of experiment.

Tab. 2 - Comparison between Ultimate Strengths by Experiment and Theory

		Ultimate Strength (kN)	Ultimate Strength Ratio (%)*
Theoretical		77.4	100
Experiment		84.6	109.3
FEA	Contact	82.4	106.5
	Interface	90.3	116.7
	rbe2	98.6	127.3
*Ultimate Strength Ratio with respect to Theoretical value (%)			

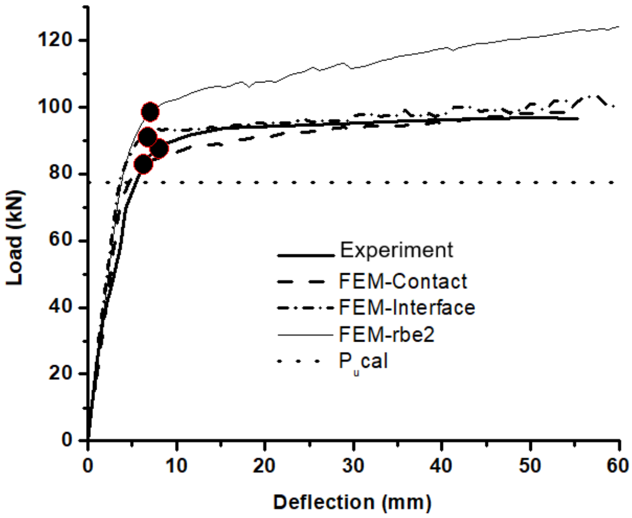

Fig. 11 – Boundary Conditions and Mesh Segmentation with rbe2 element

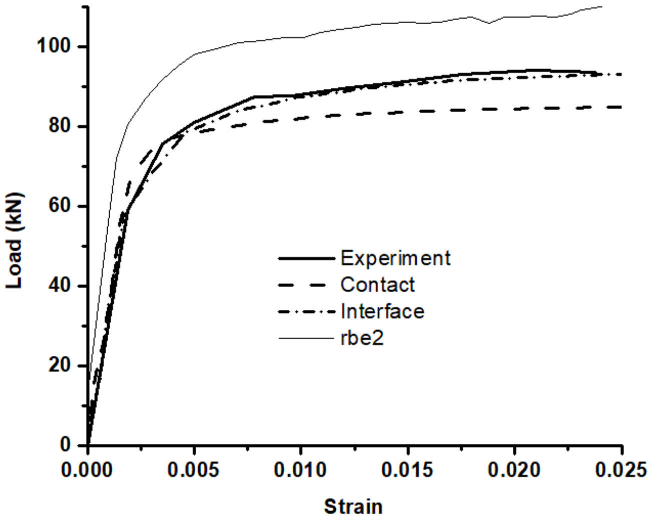

Fig. 12 – Load-Strain Relationships by Experiments and by Finite Element Analysis

Comparison of Collapse Modes by Experiments and by Finite Element Analysis

Figure 13(a) and Figure 13 (b-d) show the collapse mode of specimen by experiment and by FEA. It appears that the collapse shape of the FEA results is almost similar to the experimental results. In the experimental results there is local buckling near the loading point as shown in Figure 14(a). FEA using contact and rbe2 element did not show any local buckling near the loading point. However, FEA using interface element shows local buckling near the loading point as shown in Figure 14(b).

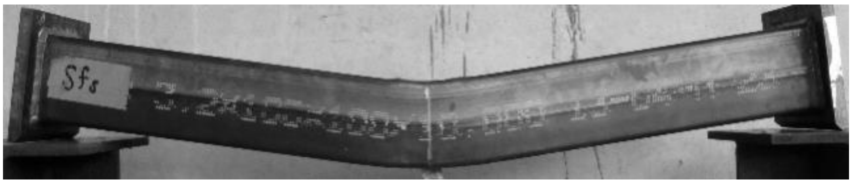

(a) Experiment

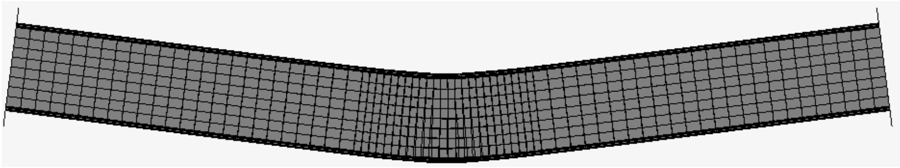

(b) Contact Analysis

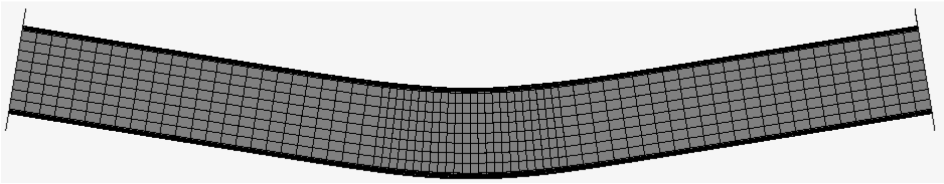

(c) rbe2 Element

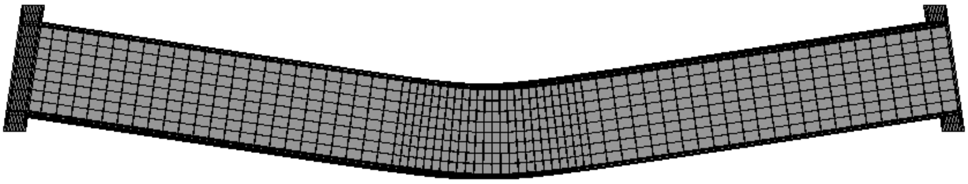

(d) Interface Element

Fig. 13 – Collapse Modes by Experiments and by Finite Element Analysis

(a) Experiment

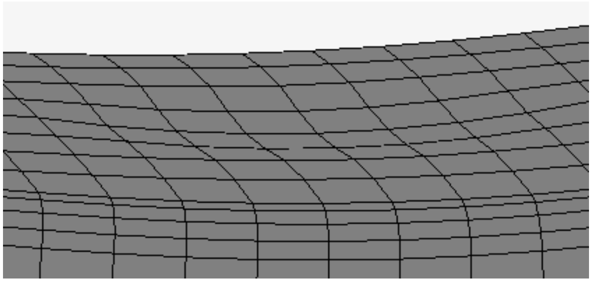

(b) Interface Element

Fig. 14 – Zoom in of Upper-side of the Beam

DOI 10.14311/CEJ.2020.02.0012

CONCLUSION

From the limited research reported in the paper, it can be concluded as follows:

1. The proposed FEA model using interface element and contact analysis can generally model the experiment of the concrete filled steel tube beam. However, the FEA model using rbe2 element is stiffer than others FEA models because the rbe2 element add the stiffness of concrete and steel.
2. The load-deflection results of the FEA model using interface element and contact analysis can be considered coincide with the experimental results. However, FEA model using rbe2 element is higher than others FEA models.
3. The load-strain results of the FEA model using interface element is matching with the experimental results. The strain of FEA model using contact analysis is lower than that of experimental results. The strain of FEA model using rbe2 element is higher than that of experimental results.
4. The collapse modes are basically identical as that of the experimental are almost identical
5. The local buckling of specimen near the loading point can be modelled only in FEA model using interface element.

ACKNOWLEDGEMENTS

We thank to Prof. Akihiko Kawano and Assoc. Prof. Shintaro Matsuo of Department Architecture, Kyushu University for supporting this research through the research facility.

REFERENCES

[1] Y. Zhang, C. Xu, X. Lu., 2007. Experimental Study of Hysteretic Behaviour for Concrete-filled Square Thin-walled Steel Tubular Columns. Journal of Constructional Steel Research, 63(3), 317-325

[2] Y. C.Tang, L. J. Li, W. X. Feng, F. Liu, B. Liao., 2017. Seismic Performance of Recycled Aggregate Concrete–filled Steel Tube Columns. Journal of Constructional Steel Research, 133, 112-124

[3] X. S.Shi, Q. Y.Wang, X. L.Zhao, F. G.Collins., 2015. Structural Behaviour of Geopolymeric Recycled Concrete Filled Steel Tubular Columns under axial loading. Construction and Building Materials, 81, 187-197

[4] Y. F.An, L. H.Han, C.Roeder., 2014. Flexural Performance of Concrete-encased Concrete-filled Steel Tubes. Magazine of Concrete Research, 66(5), 249-267

[5] G.Li, D.Liu, Z.Yang, C.Zhang., 2017. Flexural Behavior of High Strength Concrete Filled High Strength Square Steel Tube. Journal of Constructional Steel Research, 128, 732-744

[6] C. C.Hou, L. H.Han, Q. L.Wang, C. Hou., 2016. Flexural behavior of circular concrete filled steel tubes (CFST) under sustained load and chloride corrosion. Thin-Walled Structures, 107, 182-196

[7] M. Elchalakani, X. L. Zhao,R. Grzebieta., 2000. Concrete-filled Circular Steel Tubes Subjected to Pure Bending. Journal of Construction Steel Research, 57:1141-1168

[8] A.Karrech, M.Elchalakani, H.Basarir., 2017. Finite Element Modelling of Concrete Filled Steel Tubes Subjected to Static Pure Bending. In H. Hao, & C. Zhang (Eds.),Mechanics of Structures and Materials XXIV: Proceedings of the 24th Australian Conference on the Mechanics of Structures and Materials (Vol. 1, pp. 143-148). London

[9] F. K.Idan., 2017. Finite Element Analysis of Concrete-filled Aluminum tube columns. International Journal of Applied Engineering Research, 12(12), 3054-3062

[10] S.Arivalagan, S.Kandasamy., 2010. Finite element analysis on the flexural behaviour of concrete filled steel tube beams. Journal of Theoretical and Applied Mechanics, 48(2), 505-516

[11] Z.Ting, C.Zhihua, L.Hongbo., 2011. Nonlinear finite element analysis of concrete-filled steel tubular column. In Electric Technology and Civil Engineering (ICETCE), 2011 International Conference on (pp. 2396-2399). IEEE

[12] P. K.Gupta, H.Singh., 2014. Numerical study of confinement in short concrete filled steel tube columns. Latin American Journal of Solids and Structures, 11(8), 1445-1462

[13] M. H.Mollazadeh, Y. C. Wang., 2014. New insights into the mechanism of load introduction into concrete-filled steel tubular column through shear connection. Engineering Structures, 75, 139-151

[14] Wenchao, L., Wanlin, C., Qiyun, Q., Lele, R. and Ruwei, W., 2018. Study on the Seismic Performance of Recycled Aggregate Concrete-filled Lightweight Steel Tube Frame with Different Assembly Joints. Civil Engineering Journal-Stavebni Obzor, 3.

[15] MSC. MARC., 2012. User’s Guide, MSC. Software Corporation

[16] M. K.Effendi, A.Kawano., 2017. A study on the static and impact structural behavior of concrete filled steel tubular members under Tsunami flotsam collision. In AIP Conference Proceedings (Vol. 1818, No. 1, p. 020011). AIP Publishing

[17] MSC. MARC., 2012. Volume B, MSC. Software Corporation

[18] MSC. MARC., 2012. Volume A, MSC. Software Corporation

[19] Architectural Institute of Japan (AIJ)., 2008. Recommendations for design and construction of concrete-filledsteeltubular structures (in Japanese)

[20] M. Eslami, H. Namba., 2014. Effects of width-to-thickness ratio of RHS column on the elastoplasticbehavior of composite beam, Memoirs of the GraduateSchools of Engineering and System Informatics Kobe University, No.6